water

Article

Operational Risk Assessment of Check Dams in Ningxia Considering the Impact of Extreme Precipitation in the Future

Yujie Yang , Shengdong Cheng *, Zongping Ren , Zhanbin Li and Lu Jia

State Key Laboratory of Ecological Water Conservancy in Northwest Arid Areas, Xi'an University of Technology, Xi'an 710048, China; 1220412028@stu.xaut.edu.cn (Y.Y.); renzongping@163.com (Z.R.); zhanbinli@162.com (Z.L.); xiamuxingyi94@163.com (L.J.)

* Correspondence: chengsd@xaut.edu.cn

Abstract: To analyze the operation risk of check dams under extreme precipitation conditions, taking Ningxia area as an example, this paper carried out a risk assessment of check dams under extreme precipitation conditions in Ningxia through data collection, hydrological statistics, numerical simulation, and other methods. The conclusions are the following: (1) By the end of 2020, about 40% of the silt reservoir capacity of check dams in various water and soil conservation zones in Ningxia has been accumulated. During 1966–2020, the extreme precipitation and frequency of extreme precipitation in Ningxia increased while the intensity of extreme precipitation decreased. The extreme precipitation in Ningxia increased year by year and lasted longer. (2) Under two future scenarios of RCP4.5 (the full name of RCP is Representative Concentration Pathway) and RCP8.5, the extreme precipitation threshold in Ningxia is gradually decreasing from south to north. Extreme precipitation in the future will bring high risk to the operation of check dams in Ningxia. The results of this paper can provide a scientific basis for the operation and management of check dams in Ningxia.

Keywords: extreme precipitation; Ningxia check dams; operational risk assessment; climate model

Citation: Yang, Y.; Cheng, S.; Ren, Z.; Li, Z.; Jia, L. Operational Risk Assessment of Check Dams in Ningxia Considering the Impact of Extreme Precipitation in the Future. *Water* **2024**, *16*, 258. https://doi.org/10.3390/w16020258

Academic Editors: Ling Zhang and Xiaojun Liu

Received: 20 December 2023
Revised: 5 January 2024
Accepted: 7 January 2024
Published: 11 January 2024

1. Introduction

As an effective soil and water conservation facility, check dams can effectively intercept and store floods, cement sand, and silt for farmland in the Loess Plateau region with severe soil erosion [1–4]. However, due to the fact that most of the existing medium-sized and above check dams were built in the 1960s and 1970s, their supporting flood discharge facilities are not complete, and the flood control standards are not high, which cannot meet the flood control requirements of current engineering construction. For example, in July 2017, the Wuding River Basin in Shaanxi Province experienced a once-in-a-century rainfall with a maximum daily rainfall of 218.4 mm, resulting in the destruction of 337 silt dams in Suide County by floods [5]. The various situations of precarious check dams pose a threat to the safe operation of the project to varying degrees. If the removal or reinforcement measures are not timely, not only will the main building of the project be damaged, but it will also endanger the life and property safety of downstream residents [6].

In recent years, with the increase in temperature and precipitation in the northwest region of China [7,8], the heat resources in the Ningxia Hui Autonomous Region located in the eastern part of the region have been ever more abundant. At the same time, the amount of evapotranspiration has also increased, resulting in an increase in extreme precipitation events in Ningxia, and the precipitation pattern has undergone subtle changes [9–11]. The non-stationary changes caused by extreme precipitation may cause a certain degree of damage to the infrastructure of water conservancy construction projects that have been in use for a long time, such as earth and rock dams and check dams, and even pose a risk of failure [12]. Therefore, predicting whether impending climate change will affect its reliability and other safety issues is urgent.

The future situation of extreme precipitation is no longer optimistic, but there are few scholars evaluating its impact on dam operation risk. Mallakpour et al. in the United States [13] used the calculation method of historical and predicted flood return periods to analyze the potential changes in the hydrological failure risk of major dams in California under the background of climate warming, and estimated the probability of the hydrological failure of dams. As for Chinese dams, some scholars [12] have calculated the degree to which extreme precipitation intensity exceeds the dam design intensity through non-stationary GP distribution, in order to analyze the potential impact level (R) of non-stationary changes in extreme precipitation on the operational risk of Chinese dams.

Since most of these studies have not mentioned the impact of future extreme precipitation on the operational risk of check dams, this article refers to the above research methods and ideas; that is, taking Ningxia check dams as the research object, using the CMIP5 model to simulate future extreme precipitation data, using the non-stationary GP distribution to analyze the future changes of extreme precipitation in Ningxia under different climate scenarios, and evaluating the operational risks of Ningxia check dams under extreme precipitation conditions and providing valuable suggestions for the management and maintenance of check dams in the Ningxia region in the future. I hope to be able to provide assistance in the operation and management of check dams in Ningxia, to ensure their safety and functionality, and to cope with future climate change.

2. Materials and Methods

2.1. Study Area

The Ningxia Hui Autonomous Region (hereinafter referred to as Ningxia) is located in the middle and upper reaches of the Yellow River in northwest China, covering a total area of 66,400 km^2 with a distance of 456 km from north to south and about 250 km from east to west. Situated at the junction of the Loess Plateau and the Inner Mongolian Plateau, the average altitude of the whole territory is generally more than 1000 m, and the overall terrain is high in the south and low in the north. The average annual precipitation in the entire region ranges from 150 mm to 600 mm, with an average annual precipitation of around 300 mm. The geographical location and elevation of Ningxia are presented in Figure 1.

The soil erosion in Ningxia roughly includes two types: hydraulic erosion and wind erosion. As of the end of 2020, the total area of soil erosion in the entire region was 15,687.4 km^2, accounting for 23.6% of the total land area of the region, and a decrease of 201.1 km^2 compared to 2019 and a decrease of 1.3%. Among them, the hydraulic erosion area is 10,680.9 km^2, accounting for 68.1% of the soil erosion area, and the wind erosion area is 5006.6 km^2, accounting for 31.9% of the soil erosion area. According to the functional zoning of soil and water conservation, Ningxia is divided into 7 functional zones for soil and water conservation, namely Zone I—Key Prevention Area for Helan Mountain and Water Erosion, Zone II—Potential Key Prevention Area for Wind Erosion in Yinchuan Plain, Zone III—Key Control Area for Wind and Water Erosion in Arid Grassland of Hilly Plateau, Zone IV—Key Prevention Area for Liupan Mountain and Water Erosion, Zone V—Key Control Area for Water Erosion in Loess Hilly Gully and Residual Plateau, Zone VI—Key Control Area for Water Erosion in Loess Hilly and Gully, and Zone VII—Key Management Area for Water Erosion Intersection in Huangtu Hilly Gully and Phoenix (Figure 2). In order to develop more scientific measures for the operation and management of silt dams in various regions, the precipitation and silt dam situation will be analyzed in the context of soil and water conservation zoning in Ningxia.

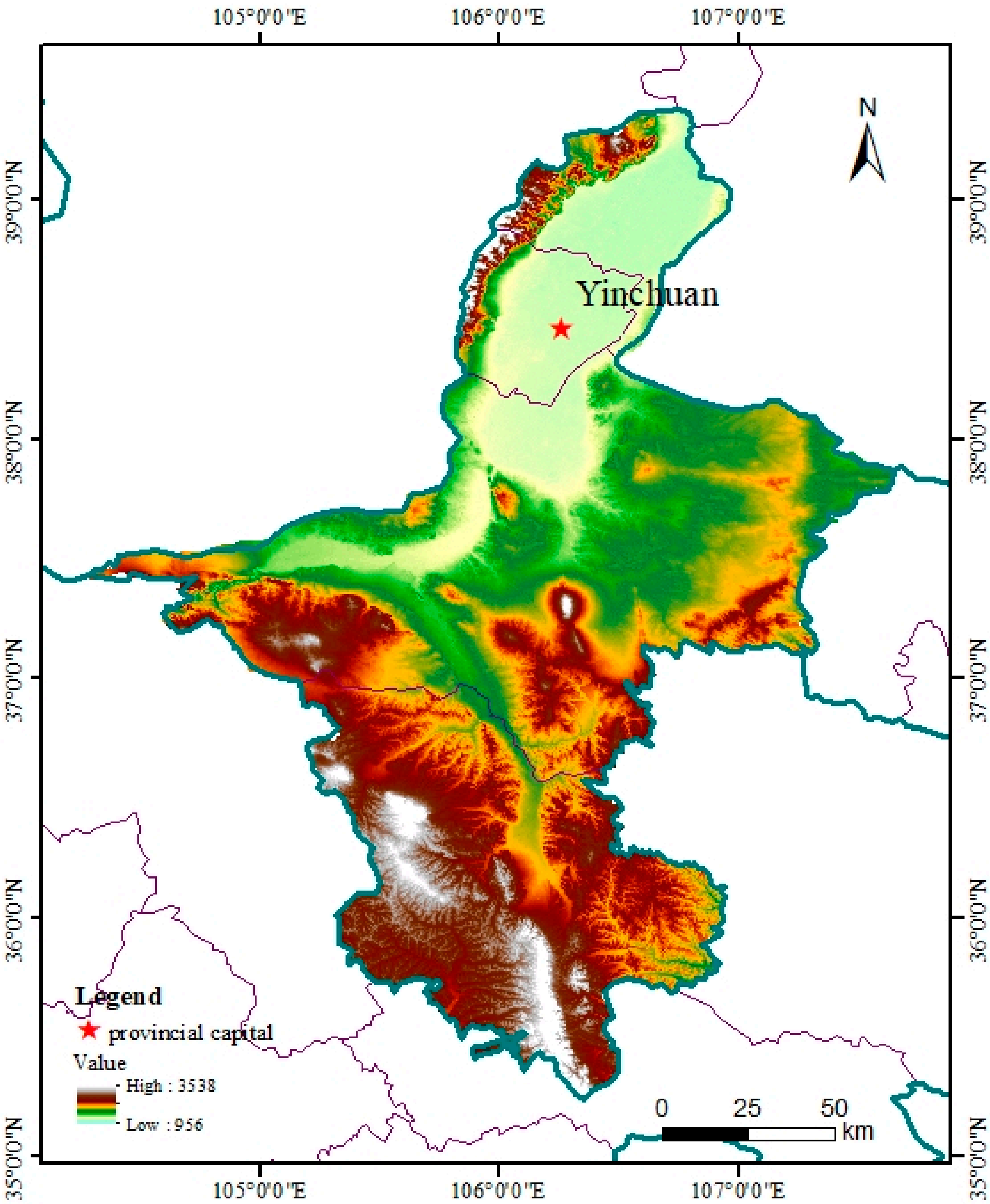

Figure 1. Geographical location and elevation of Ningxia.

2.2. Data Sources

The diverse data information of check dams in the Ningxia region mainly comes from the latest survey and statistics of check dams in Ningxia (2020), organized and compiled by the Soil and Water Conservation Monitoring Station of Ningxia Hui Autonomous Region.

The daily precipitation data of 20 stations in Ningxia from 1966 to 2020 are sourced from the China Meteorological Science Data Sharing Service Network (http://cdc.cma.gov.cn/) National meteorological station data provided. For future precipitation, accessed on 5 June 2020 to obtain the CMIP5 model data from https://esgf-node.llnl.gov/projects/esgf-llnl/, and the YSU-RSM climate model with good applicability to the Ningxia region is selected [14]. The content covers historical simulations from 1980 to 2005 and daily precipitation data under RCP4.5 (the full name of RCP is Representative Concentration Pathway, i.e., by 2100, greenhouse gas concentration corresponds to a radiation forcing of 4.5 W/m^2) and RCP8.5 (i.e., by 2100, greenhouse gas concentration corresponds to a radiation forcing of 8.5 W/m^2) scenarios from 2006 to 2050.

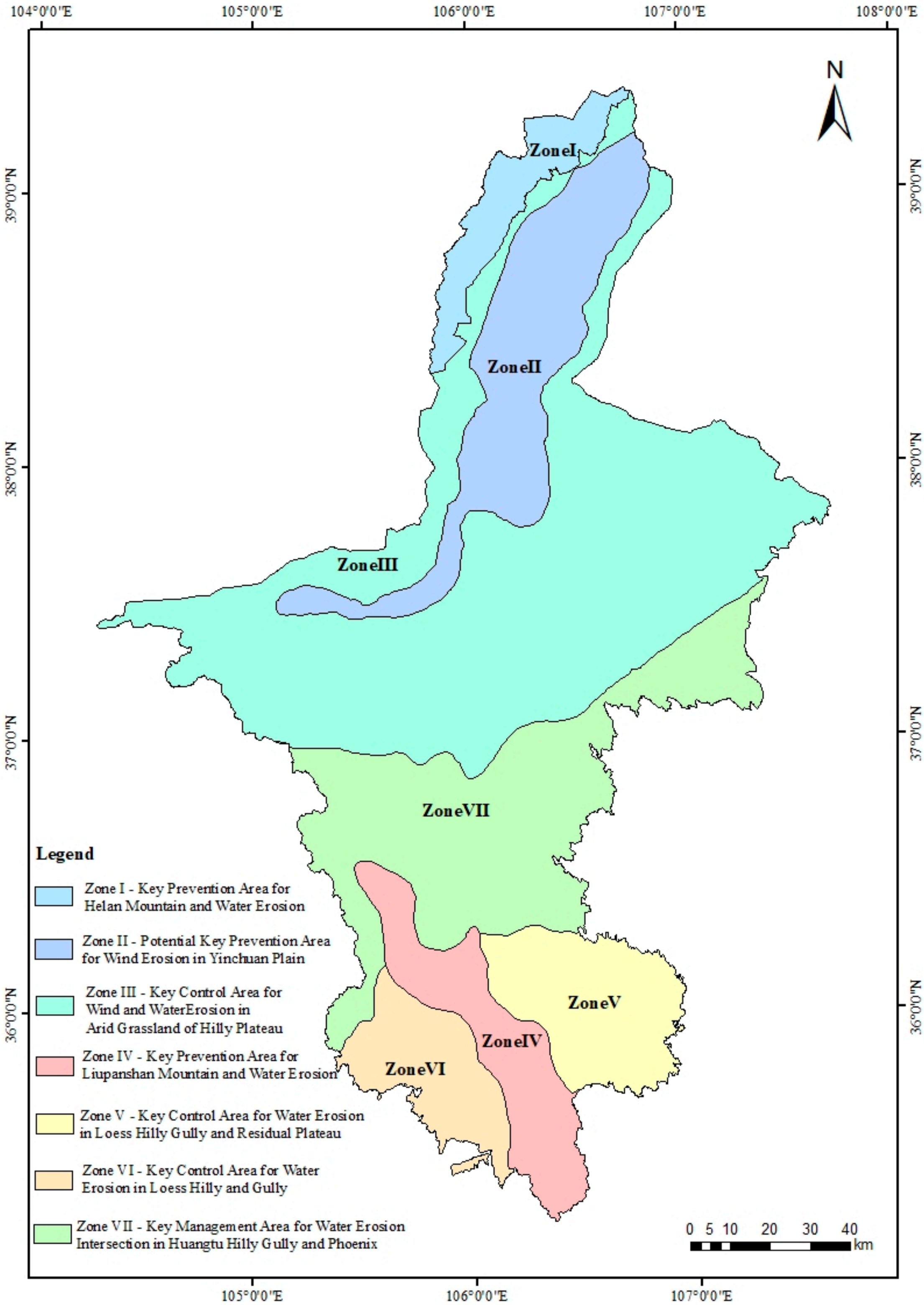

Figure 2. Functional zoning map of soil and water conservation in Ningxia (including county and district names).

2.3. Analysis Methods

2.3.1. Analysis Methods for Extreme Precipitation Events

1. Determination of extreme precipitation events and extreme precipitation indicators

This article defines extreme precipitation using 95% percentile values [15,16]. Consider adopting the following three indicators to describe the basic characteristics of extreme precipitation, and the definitions of each indicator are shown in Table 1.

Table 1. Extreme precipitation indicators and their definitions.

Serial Number	Symbol	Indicator Name	Define	Unit
1	P	Extreme precipitation	The total annual precipitation of extreme precipitation events	mm
2	F	Extreme precipitation frequency	The number of days that extreme precipitation events occur each year	d
3	I	Extreme precipitation intensity	The ratio of extreme precipitation to extreme precipitation days	mm/d

2. Trend analysis of changes

Use the linear regression method to analyze the trend of extreme precipitation events in the Ningxia region. The linear regression equation is shown in Equation (1) [17]:

$$\hat{y} = \hat{a} + \hat{b}t \quad (1)$$

In the formula, $\hat{y}$ is the extreme precipitation indicators; $\hat{a}$ is the regression intercept; and the regression coefficient $\hat{b}$ represents the variable $\hat{y}$ trend inclination. When $\hat{b}$ is positive, it indicates that as time t increases, $\hat{y}$ shows an increasing trend; when $\hat{b}$ is negative, it indicates that as time t increases, $\hat{y}$ shows a decreasing trend; and t is the time range.

3. Deviation correction of pattern data

This article adopts the Delta bias correction method to correct the bias of pattern data [18,19]. The formula is shown in Equation (2):

$$P_{station,f,daily} = P_{GCM,f,daily} \cdot \frac{\overline{P_{station,h,monthly}}}{\overline{P_{GCM,h,monthly}}} \quad (2)$$

In the formula, $P_{station,f,daily}$ are the daily precipitation data of GCM under future scenarios after down scaling; $P_{GCM,f,daily}$ are the original daily precipitation data of GCM under future scenarios; $\overline{P_{station,h,monthly}}$ is the annual monthly average precipitation of meteorological stations in historical periods; and $\overline{P_{GCM,h,monthly}}$ is the original monthly average precipitation of GCM during the historical period.

2.3.2. Indicators and Calculation Methods for Evaluating Operational Risks

1. Evaluation indicators

This article uses the potential impact level R to conduct an operational risk assessment on check dams in the Ningxia region. The definition of this evaluation index is shown in Equation (3) [12]:

$$R(t) = \frac{N(t) - S}{S} \times 100\% \quad (3)$$

In the formula, $R(t)$ is the potential impact level, %; $N(t)$ is the precipitation intensity at time t calculated from the local non-stationary GP distribution, mm; and S is the design strength of the dam body calculated from the locally stable GP distribution, mm.

From Equation (3), we can see that compared to the design intensity, the greater the extreme precipitation intensity in the future, the greater the impact on the check dam.

Therefore, the potential impact level $R(t)$ can more intuitively represent the possible influence of extreme precipitation changes on the operation process of check dams.

The critical value of the potential impact level $R(t)$ can be determined based on the anti-skid safety factor of the check dam [12]. Considering that the storage capacity of check dams will show significant siltation over time, the design standards for various types of check dams should be adjusted in future scenarios. The diagnostic values of the potential impact levels $R(t)$ for different types of check dams are listed in Table 2.

Table 2. List of critical values for potential impact levels $R(t)$ of different types of check dams.

Type of Check Dam	Original Design Standard (Return Period T_{R0}/a)	The Anti-Skid Safety Factor for Normal Use	Adjusted Design Standards (Return Period T_R/a)	$R(t)$ Critical Value (%)
Key dam	20–30	1.25	10–20	20
Medium sized dam	20–10	1.20	10–20	20
Small dam	10–20	1.20	5–10	15

2. Method of calculation

- Stable GP distribution

For the calculation of the design strength S of the dam body, it can be seen from Equation (3) that the locally stable GP distribution is used to analyze the design strength of different types of check dams near numerous stations in Ningxia. Simulate future extreme precipitation from 2016 to 2050 using two scenarios in the YSU-RSM climate model for each site. Based on the adjusted design standards for different types of check dams, calculate the corresponding design values at the design frequency, which will serve as the design strength of the check dams. Due to the use of the ultra-quantitative method [18] for extreme precipitation data, the relationship between the design frequency and the recurrence period of the ultra-quantitative method is shown in Equation (4):

$$T_R = \frac{1}{\bar{k} \cdot p} \tag{4}$$

In the formula, T_R is the return period of the ultra-quantitative method, a; $\bar{k}$ means the average number of selected data per year for the ultra-quantitative method; and p is the design frequency, %.

- Non-stationary GP distribution

According to Equation (3), the upcoming extreme precipitation intensity $N(t)$ of the different types of check dams near each station can be calculated using local non-stationary GP distribution. Similar to the method of calculating the design strength S of the dam body, it is assumed that the model simulates the extreme precipitation from 2016 to 2050, which follows a fixed parameter GP distribution every five years. The design values of different types of check dams at corresponding design frequencies are analyzed every five years, and this is used as the extreme precipitation intensity of the check dams during these five years.

3. Results and Analysis

3.1. Spatial Characteristics of the Distribution of Check Dams in the Ningxia Region

3.1.1. Spatial Distribution Characteristics of Check Dams

As of the end of 2020, there were a total of 1119 check dams built in Ningxia, of which 324 were backbone dams with a storage capacity of over 500,000 square meters, accounting for 29.0% of the total number of check dams. There are 369 medium-sized check dams with a storage capacity between 100,000 and 500,000 square meters, accounting for 33.0% of the total number of check dams. There are 426 small check dams with a storage capacity between 10,000 and 100,000 square meters, accounting for 38.1% of the total number of check dams. The distribution of check dams in Ningxia is illustrated in Figure 3. It can be seen that check dams are mainly distributed in Zone III (Yanchi County, Shapotou District, and Lingwu City), Zone V (Yuanzhou District and Pengyang County), Zone VI (Xiji County and Longde County), and Zone VII (Tongxin County and Haiyuan County).

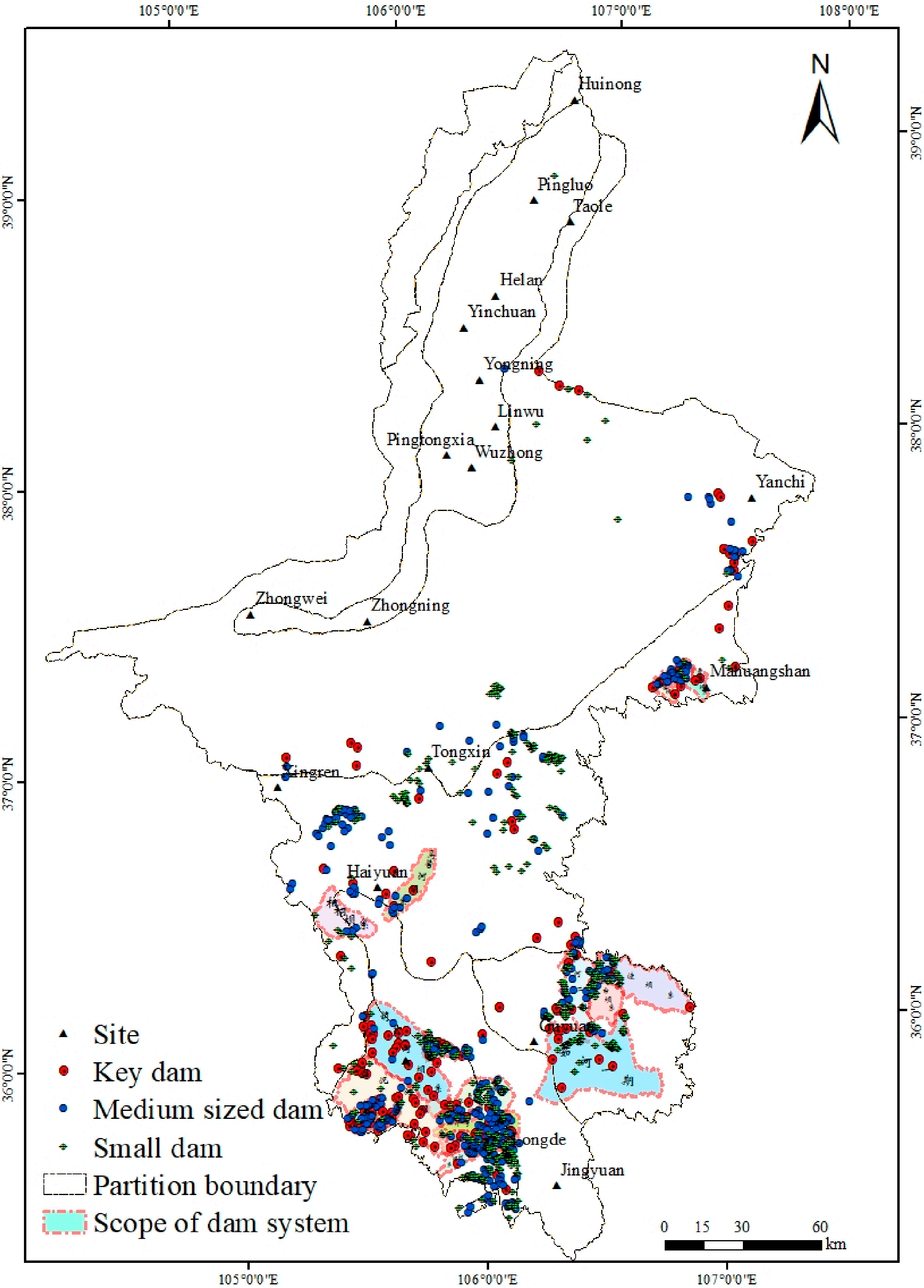

Figure 3. Distribution map of check dams in Ningxia.

The distribution of backbone dams, medium-sized check dams, and small check dams in various cities and counties (districts) is shown in Figure 4, which shows the number of check dams constructed according to the classification of soil and water conservation zones. Overall, the maximum number of check dams in Zone VI is 448, followed by 319 in Zone V and 187 in Zone VII, while the minimum number of check dams in Zone III is 156. It can be inferred that the key area for the construction of check dams in Ningxia is the loess hill and gully areas.

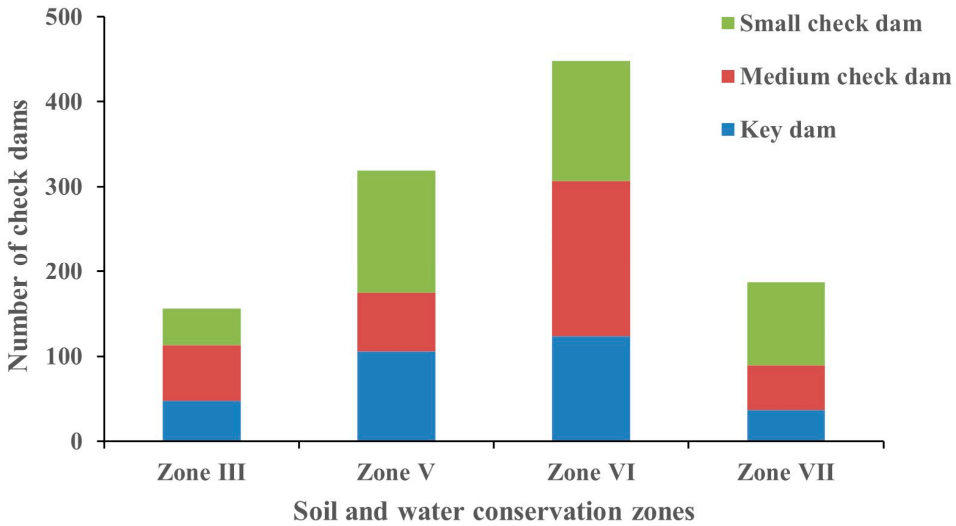

Figure 4. Statistics of the number of check dams constructed in different soil and water conservation zones in Ningxia.

3.1.2. Current Situation of Sedimentation in Check Dams

Analyzing the siltation situation of the silt dam is beneficial for understanding the operational status of the silt dam, providing technical support and a decision-making basis for the planning and design, risk prevention and control, operation management, and benefit evaluation of the silt dam. The total control area of backbone dams and medium-sized check dams in Ningxia is 4561.0 km^2, with a designed total storage capacity of 412.245 million m^3, including a flood control storage capacity of 243.078 million m^3, siltation storage capacity of 169.167 million m^3, siltation storage capacity of 63.264 million m^3, and remaining siltation storage capacity of 105.903 million m^3. In the current situation of siltation in countless districts of Ningxia (Figure 5), the proportion of the control area in Zone III is relatively large. However, for aggregate storage capacity, flood control storage capacity, siltation storage capacity, and already silted storage capacity, the proportion of Zones III and VI is relatively large. Overall, the silted storage capacity of the check dams in each zone accounts for about 40% of the silted storage capacity, while the remaining silted storage capacity accounts for about 60%.

3.2. Analysis of Extreme Precipitation Trends in the Ningxia Region

3.2.1. Analysis of Historical Precipitation Data

1. Threshold distribution

The distribution map of extreme precipitation thresholds during the historical period of Ningxia (Figure 6) shows that the areas with higher thresholds are mainly located in the southeast of Zone IV and Zone V, while the smaller areas are in the west of Zone II and Zone III. The general distribution trend is slightly decreasing from southeast to northwest. In Zone IV and V, the extreme precipitation thresholds for Jingyuan and Guyuan are 23.2 mm and 19.9 mm, respectively, while in Qingtongxia in Zone II, Zhongwei in Zone III, and Xingren in Zone VII, they are all below 15.29 mm. This spatial distribution is basically consistent with the distribution of the average annual precipitation in the climate (Figure 7).

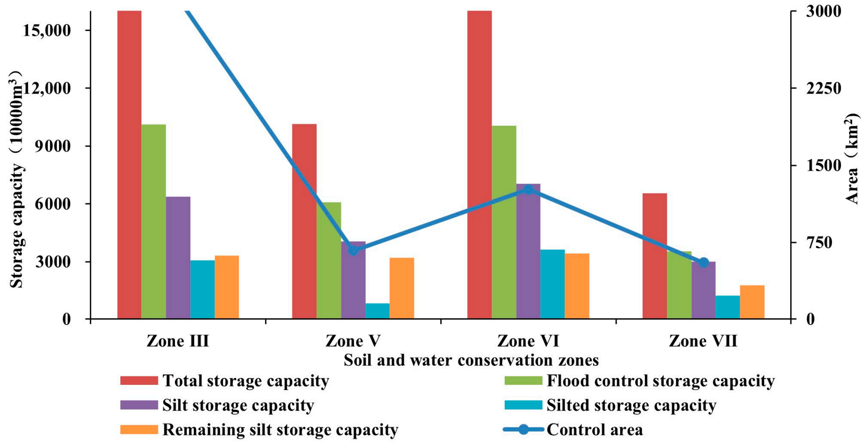

Figure 5. Statistical chart of the current siltation status indicators of siltation dams in various districts of Ningxia.

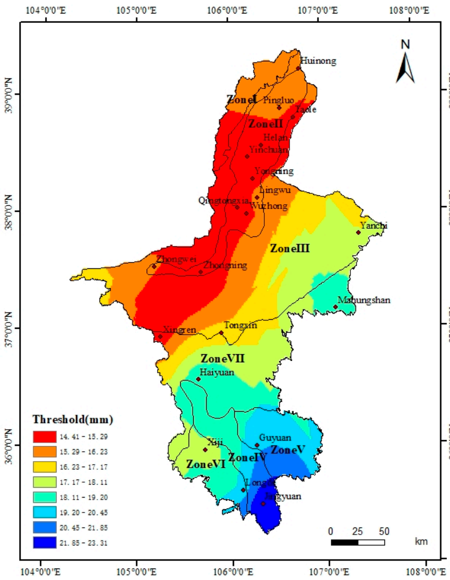

Figure 6. Extreme precipitation threshold distribution map.

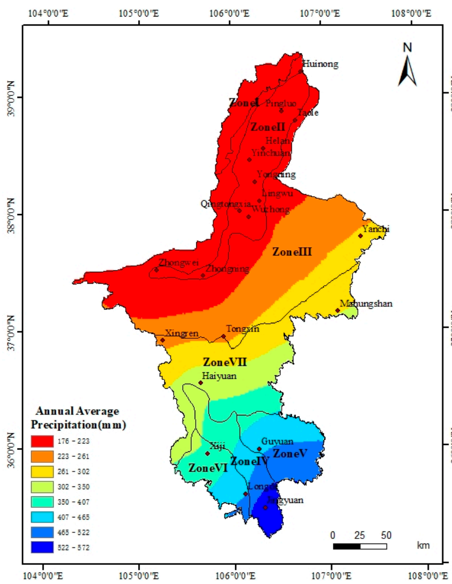

Figure 7. Distribution map of annual average precipitation in Ningxia from 1966 to 2020.

2. The spatial distribution of extreme precipitation index trends

It can be observed in Figure 8a that the extreme precipitation in most regions of Ningxia from 1966 to 2020 was mainly increasing, with a change range of −0.32 to 0.85 mm/a. Among them, Zhongning in Area II, Jingyuan in Area IV, Xiji in Area VI, Ma Mount Huangshan in Area VII, and other regions showed a slightly decreasing trend, with a relatively large decrease range of 0.32 mm/a in Zhongning, and an increasing trend in other regions. Pingluo in Area II was the largest, reaching 0.85 mm/a. According to the approximate distribution in the graph, except for the VI zone where the extreme precipitation from 1966 to 2020 showed a decreasing trend, all other zones had stations with an increasing tendency.

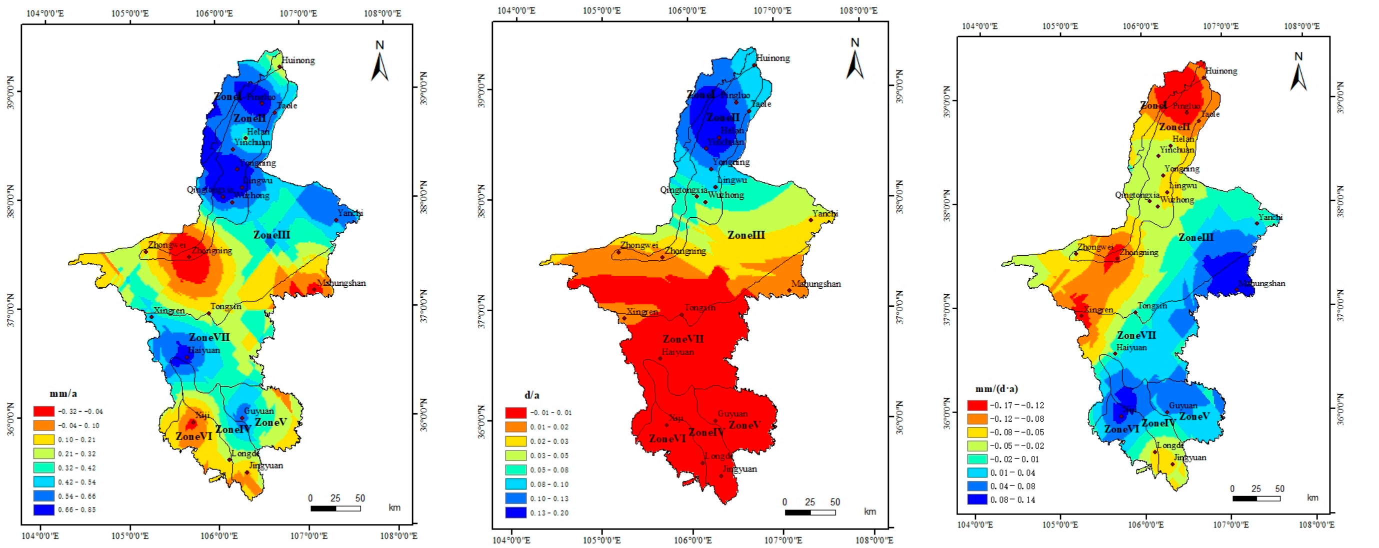

(**a**) (**b**) (**c**)

Figure 8. Distribution map of extreme precipitation index tendency in Ningxia from 1966 to 2020: (**a**) extreme precipitation; (**b**) extreme precipitation frequency; (**c**) extreme precipitation intensity.

The distribution of the extreme precipitation frequency tendency rate (Figure 8b) is approximately the same as the distribution of the extreme precipitation tendency rate. Except for Zhongning in Zone II, Xiji in Zone VI, and Ma Mount Huangshan in Zone VII, the distribution of the extreme precipitation frequency tendency rate shows an increasing trend in most other regions, with a trend rate of −0.01~0.20 d/a. Helan in Zone II has the most obvious increasing trend, with an increase rate of 0.20 d/a.

From Figure 8c, we can get the tendency rate of extreme precipitation intensity in Ningxia. Except for Zhongning and Helan in Area II, and Ma Mount Huangshan in Area VII, the trend is increasing, and most other areas are decreasing, in which Pingluo in Area II decreases by 0.17 mm/(d·a), indicating that the extreme precipitation and the frequency of extreme precipitation events in most water and soil conservation areas in Ningxia are increasing from 1966 to 2020, but the extreme precipitation intensity is decreasing.

3.2.2. Prediction of Future Change Trends

1. Result analysis under RCP4.5 scenario

- Threshold distribution

As shown in Figure 9, the extreme precipitation threshold of each partition station exceeds 19.46 mm, and the distribution range is consistent with the historical extreme precipitation threshold, which gradually increases from the northwest of Ningxia to the southeast; the central guard in Zone II is the smallest, 19.46 mm, but larger than its historical analysis of 14.56 mm, and the largest Jingyuan in Zone IV is 38.42 mm, which is also greater than its historical analysis of 23.2 mm. This indicates that under the RCP4.5 scenario, the threshold for extreme precipitation in diverse regions of Ningxia is increasing.

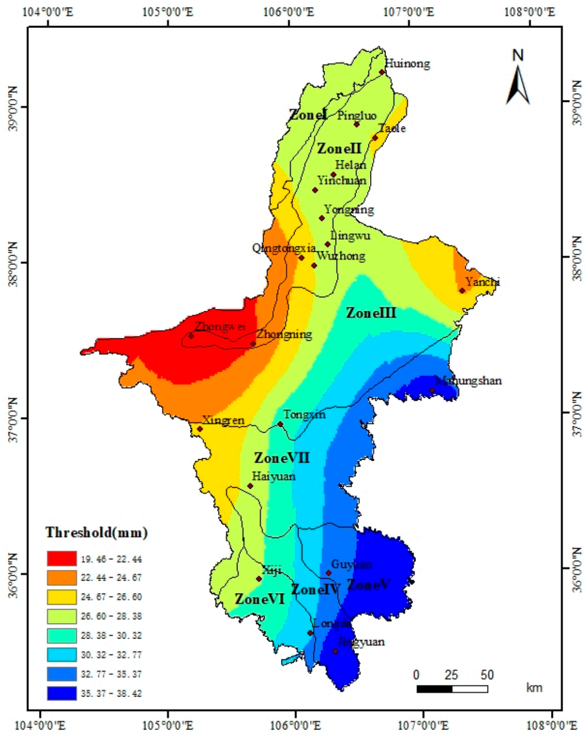

Figure 9. Distribution of extreme precipitation threshold under RCP4.5 scenario.

- The spatial distribution of extreme precipitation index trends

From 2006 to 2050, the utmost precipitation in most areas of Ningxia showed an increasing trend (see Figure 10a), with a range of −1.18 to 5.55 mm/a. Among them, the stations in Zone II showed a decreasing trend, with Wuzhong showing a relatively larger decrease of 1.18 mm/a, while the other zones showed an increasing trend. Jingyuan in Zone IV had the largest increase of 5.55 mm/a. From the rough distribution in the figure, the tendency rate of extreme precipitation under the RCP4.5 scenario also shows a gradually increasing distribution from north to south.

The extreme precipitation frequency trend of most stations in the region is positive (Figure 10b), ranging from −0.020 to 0.117 d/a. Among them, Helan, Yongning, Lingwu, and Wuzhong in Zone II have negative values, while the trend rates of additional stations are greater than 0. The inclination rate in the central and northern regions (from Zone I to Zone III) is relatively low, and except for the larger values at stations such as Yinchuan, Zhongwei, and Zhongning in Zone II, the rest are generally less than 0.036 d/a. The frequency tendency of extreme precipitation in the southern region (from Zone IV to Zone VII) is generally greater than 0.036 d/a. In the RCP4.5 scenario, there is a slight increase in the frequency of extreme precipitation at each station, and it gradually increases from north to south.

The trend rate of extreme precipitation intensity at each partition site ranges from −0.22 to 0.74 mm/(d·a) (Figure 10c). Among them, the trend rates of Wuzhong and Zhongning in Zone II, as well as Yanchi and Tongxin in Zone III, are relatively small, ranging from −0.22 to −0.10 mm/(d·a), showing a decreasing trend. However, Xingren in Zone VII is relatively enormous, at 0.74 mm/(d·a). Therefore, it can be concluded that the trend rates of extreme precipitation intensity in each partition of Ningxia are relatively muted, In the RCP4.5 scenario, there is a gradually increasing distribution trend from east to west.

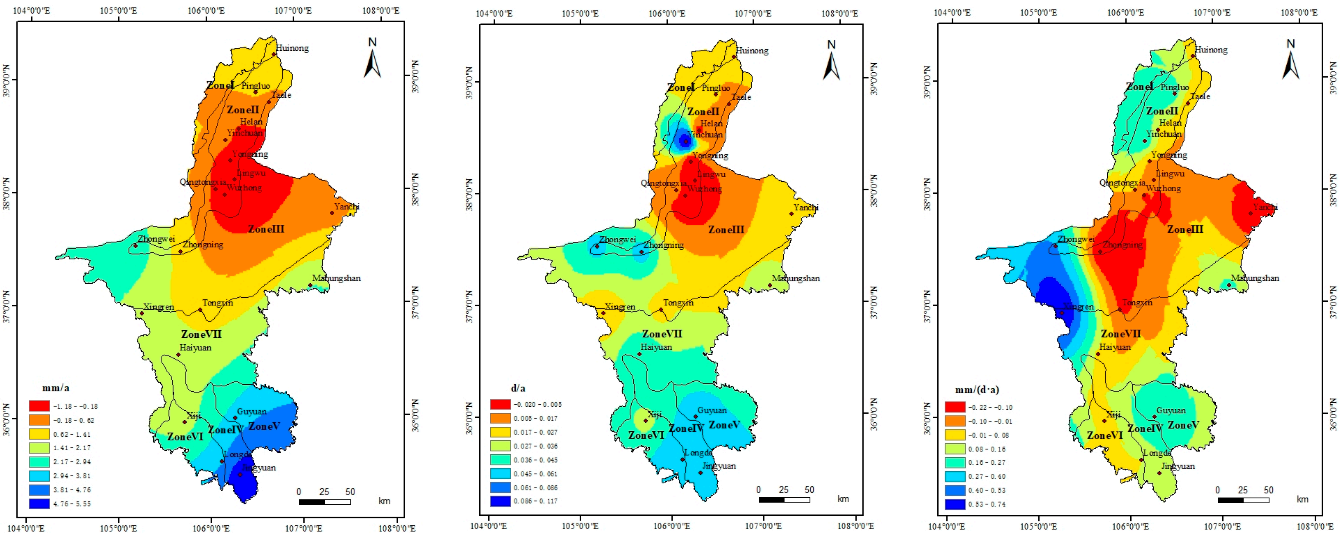

(**a**) (**b**) (**c**)

Figure 10. Distribution map of extreme precipitation index tendency in Ningxia from 2006 to 2050 under RCP4.5 scenario: (**a**) extreme precipitation; (**b**) extreme precipitation frequency; (**c**) extreme precipitation intensity.

2. Result analysis under RCP8.5 scenario
    - Threshold distribution

As shown in Figure 11, it can also be seen that the threshold values of each partition exceed the maximum historical threshold value of 19.46 mm, and the distribution situation is basically the same as the historical threshold, which increases gradually from northwest to southeast. Therefore, the extreme precipitation thresholds of various regions in Ningxia gradually increase under the RCP8.5 scenario.

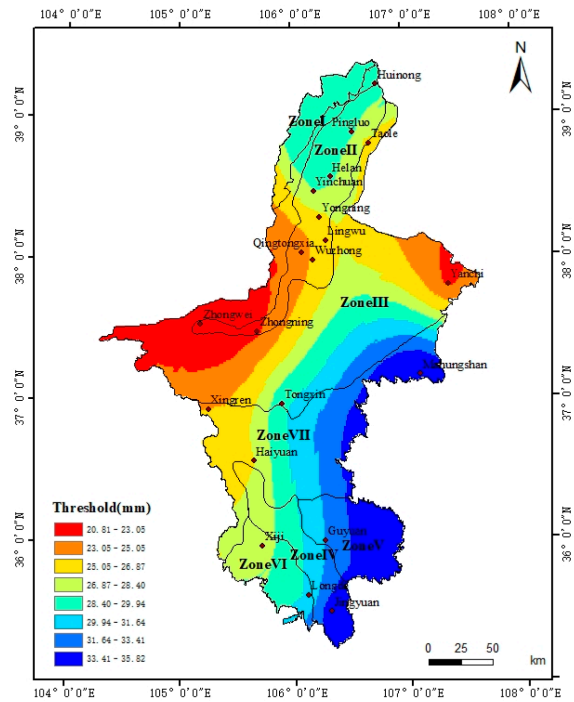

Figure 11. Distribution of extreme precipitation threshold under RCP8.5 scenario.

- The spatial distribution of extreme precipitation index trends

The tendency rate of extreme precipitation at each station in each partition is assured (Figure 12a), ranging from 0.31 to 4.85 mm/a. Among them, Zhongwei and Zhongning in Zone II, Huinong in Zone III, and Xingren in Zone VII are smaller, ranging from 0.31 to 1.00 mm/a, while Jingyuan in Zone IV and Haiyuan in Zone VII are larger, ranging from 4.00 to 4.85 mm/a.

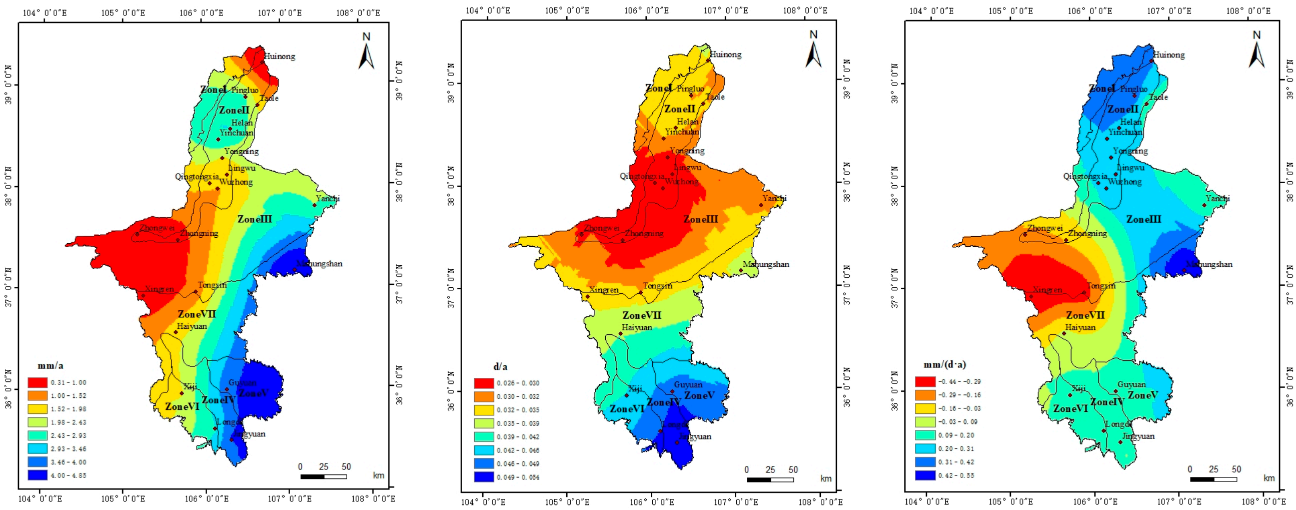

(**a**) (**b**) (**c**)

Figure 12. Distribution map of extreme precipitation index tendency in Ningxia from 2006 to 2050 under RCP8.5 scenario: (**a**) extreme precipitation; (**b**) extreme precipitation frequency; (**c**) extreme precipitation intensity.

The tendency rate of extreme precipitation frequency is also positive (Figure 12b), with stations south of Yongning in Zone II having a smaller tendency rate, ranging from 0.026 to 0.030 d/a, while Jingyuan in Zone IV and Longde in Zone VI have a larger tendency rate, ranging from 0.049 to 0.054 d/a. Under the RCP8.5 scenario, the frequency of extreme precipitation at various sub stations in Ningxia also shows an increasing trend.

The variation range of the extreme precipitation intensity tendency rate at each station is −0.44~0.55 mm/(d·a) (Figure 12c), in which Tongxin in Area III and Xingren in Area VII are smaller, between −0.44 and ~−0.29 mm/(d·a), while Ma Mount Huangshan in Area VII is the largest, at 0.55 mm/(d·a). Therefore, the extreme precipitation intensity changes in discrete zones under the RCP8.5 scenario are not entirely the same, showing a gradually increasing trend from west to east.

3.3. Risk Assessment of Check Dam Operation under Extreme Precipitation

Based on the evaluation index of the probable impact level $R(t)$ in Equation (4), analyze the operational risks of different types of siltation dams in different regions of Ningxia from 2016 to 2050 under different scenarios of RCP4.5 and RCP8.5. The latitudinal distribution map of the check dam is shown in Figure 3.

3.3.1. Evaluation Results under RCP4.5 Scenario

As shown in Figure 13, due to the lack of the construction of check dams in the northern part of Ningxia (the northern part of Zone I, II, and III), the $R(t)$ value in this area remains around 0, while it far exceeds 0 from 2026 to 2030. It is not excluded that there may be deviations in the selected evaluation methods or model simulation data. It is worth noting that the $R(t)$ near the inner guard in Zone III has been consistently above 50%, far exceeding 20%. From 2016 to 2030, the $R(t)$ in the southern part of Ningxia (from Zone IV to Zone VII) moderately increased, reaching a maximum of 35% by 2030 and gradually decreasing thereafter, but also exceeding 20%. In addition, considering that the extreme precipitation intensity in the central region of Ningxia is slightly higher than that in the southern region, from 2016 to 2050, the $R(t)$ value in the central region of Ningxia is generally higher than that in the southern region. In short, in the RCP4.5 scenario, there are certain operational risks for different types of check dams in various zones south of Zhongwei in Ningxia.

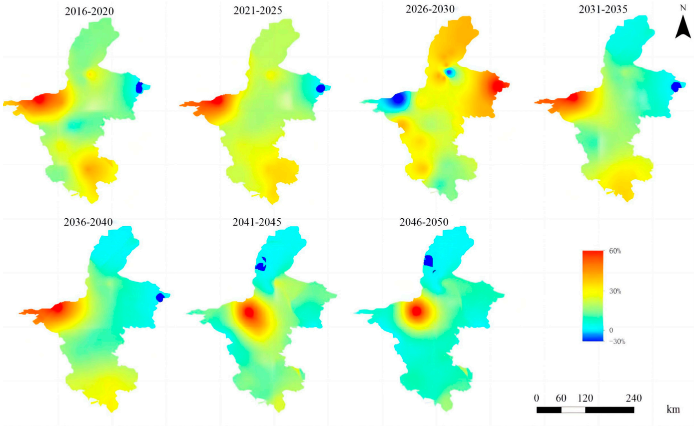

Figure 13. Changes in $R(t)$ value of potential impact level of check dams in Ningxia region under RCP4.5 scenario.

3.3.2. Evaluation Results under RCP8.5 Scenario

From Figure 14, it can be seen that the northern part of Ningxia (the northern part of Zone I, II, and III) shows a value of around 0, while the risk of the principal region varies greatly at different ages. This may also be due to the weaker applicability of the evaluation method in the fundamental region compared to the northern and southern regions. From 2021 to 2050, the $R(t)$ of most areas in the southern region (from Zone IV to Zone VI) has been almost consistently above 50%. Since 2031, the $R(t)$ of the southern and seventh regions of Zone III has also been between 10 and 20%, indicating that under the RCP8.5 scenario, the operation of different types of check dams in southern Ningxia, especially from Zone IV to Zone VI, will be affected. Overall, the operational risk of silt dams in the Ningxia region is higher under the RCP8.5 scenario.

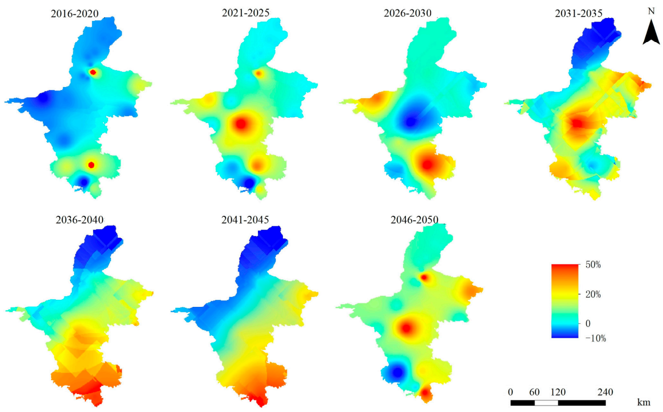

Figure 14. Changes in $R(t)$ value of potential impact level of check dams in Ningxia region under RCP8.5 scenario.

4. Discussion

4.1. Analysis of Historical Extreme Precipitation Trends

The extreme precipitation threshold in Ningxia from 1966 to 2020, determined using the percentile method, mainly shows a marginally decreasing distribution from southeast to northwest. Zhang, M.J. et al. [20] also reached similar conclusions that the annual precipitation in Ningxia from 1951 to 2008 increased from north to south. Scholars such as Chen, X.G. et al. [21] have shown that during the 45 years from 1961 to 2005, the number of days with precipitation above 25.0 mm in the summer and autumn seasons in Ningxia increased, and the frequency distribution of precipitation showed a clear trend towards a higher level of precipitation, which is consistent with the analysis results in the article.

In addition, the distribution of historical extreme precipitation thresholds in Ningxia is very close to the distribution of average annual climate precipitation, which is consistent with the study by Li, F. et al. [22]. In the view of Yang, Y. et al. [23], climate and terrain may be important factors affecting the north–south differences in extreme precipitation events, or they may be influenced by particularly significant human activities.

From the research of Fan, K. [24] and Xin, Z.B. et al. [25], it can be concluded that Ningxia belongs to an arid and semi-arid region. Once a long period of heavy rainfall occurs, it means that the surface runoff generated by natural precipitation increases or flood disasters intensify, which easily leads to urban waterlogging and soil erosion in the region. Therefore, analyzing the trend of extreme precipitation changes in the region and implementing corresponding protection and management measures can significantly reduce the losses caused by natural catastrophes.

4.2. Operational Risk Assessment of Check Dams

Ma, L. et al. [26,27] found that under the condition of a rainstorm, the blocking dam has an efficient sediment-retaining effect, but the dam with a small reservoir capacity very easily has a large siltation depth, which poses a threat to the dam body, indicating that extreme precipitation will cause dam break danger to the warping dam. Zu, Q. et al. [28] also pointed out that different types of check dams have altered susceptibility to burst debris flows caused by precipitation of different durations and frequencies. Overall, the longer the precipitation duration, the lower the precipitation frequency, and the higher the reservoir capacity, the higher the susceptibility level of debris flows formed by check dams, and the higher the risk of dam failure. Therefore, when extreme precipitation occurs, various types of check dams are given the opportunity to collapse. These studies [29] further confirm the rationality of the operative risk assessment results of check dams under extreme precipitation conditions in this paper.

At the same time, Gao, Y. et al. [30] and others pointed out that the extreme value of rainstorm is one of the important bases for the design flood of large-scale water conservancy projects. China’s Code for Design Flood Calculation of Water Resources and Hydropower Projects (SL44-2006) emphasizes that attention should be paid to the collection of extremely heavy rainstorm data in the region and adjacent areas, and the design results should be compared with the rainstorm records to check whether the design data are safe and reliable. For certain areas lacking flow data, the method of calculating design floods based on rainfall can also provide a basis for design. Therefore, the study of the rainstorm extreme value is of great significance for the planning, design, and safe operation of water conservancy projects.

5. Conclusions

(1) As of the end of 2020, there were a total of 1119 check dams in Ningxia, including 324 backbone dams, 369 medium-sized check dams, and 426 small check dams. These completed check dams are mainly located in the soil and water conservation functional zones (Zone III, V, VI, and VII) of the Loess Hilly Gully. The silted storage capacity of each zone’s check dams accounts for about 40% of the silted storage capacity, and the siltation situation is relatively serious.

(2) During the period of 1966 to 2020, the threshold for extreme precipitation in the entire Ningxia region gradually decreased from southeast to northwest, with an increase in extreme precipitation of about 0.27 mm/a, an increase in extreme precipitation frequency of about 0.10 d/a, and a decrease in extreme precipitation intensity of about −0.02 mm/(d·a). The extreme precipitation in the entire region increased year by year and its duration was prolonged.

(3) Under the two future scenarios of RCP4.5 and RCP8.5, the distribution of extreme precipitation thresholds in Ningxia is basically the same as in bygone periods. In the RCP4.5 scenario, the extreme precipitation increases approximately by 2.19 mm/a, the frequency of extreme precipitation increases roughly by 0.05 d/a, and the intensity of extreme precipitation increases approximately by 0.26 mm/(d·a). In the RCP8.5 scenario, the increase in extreme precipitation is slightly greater than in RCP4.5, while the increase in extreme precipitation frequency and intensity is slightly smaller than in RCP4.5.

(4) In the RCP4.5 scenario, the check dams south of Zhongwei in Zone III and Zone VII will be significantly affected ($R(t)$ much greater than 20%); in the RCP8.5 scenario, there is a certain degree of risk ($R(t)$ of over 20%) in the operation of check dams from Zone IV to Zone VI. Therefore, in different future scenarios, the potential impact level $R(t)$ of the siltation dams in various regions of Ningxia is much higher than the critical value of 20% (15%), and extreme precipitation will bring high risks to the siltation dams in the entire region.

Author Contributions: Conceptualization, Y.Y. and S.C.; methodology, Z.R.; software, Y.Y.; validation, Y.Y., S.C. and Z.L.; formal analysis, L.J.; investigation, S.C.; resources, Z.R.; data curation, Y.Y.; writing—original draft preparation, Y.Y.; writing—review and editing, S.C.; visualization, Y.Y.; supervision, Z.R.; project administration, S.C.; funding acquisition, Z.L. All authors have read and agreed to the published version of the manuscript.

Funding: The study was financially supported by the National Key Research and Development Program of China (Grant No. 2022YFF1300803) and the National Natural Science Foundations of China (No.52179043).

Data Availability Statement: Data will be made available upon request.

Conflicts of Interest: The authors declare that they have no known competing financial interests or personal relationships that could have appeared to influence the work reported in this paper.

References

1. Xu, X.Z.; Zhang, H.W.; Zhang, O.Y. Development of check-dam systems in gullies on the Loess Plateau, China. *Environ. Sci. Policy* **2004**, *7*, 79–86. [CrossRef]
2. Chen, Z.Y.; Li, Z.B.; Wang, Z.Y. Some thoughts on the strategic positioning of check dam construction in the Loess Plateau. *Soil. Water. Conserv. China* **2020**, *9*, 32–38. [CrossRef]
3. Ministry of Water Resources of the People's Republic of China. *Zhongguo Heliu Nisha Gongbao*; China Water & Power Press: Beijing, China, 2020.
4. Gao, H.D.; Jian, L.L.; Li, Z.B.; Xu, G.C.; Zhao, B.H. Mechanism underlying impact of check damson runoff based graph theory in the hilly-gully loess region. *Sci. Soil Water Conserv.* **2015**, *13*, 1–8. [CrossRef]
5. Yu, T.; Li, Z.B.; Chen, Y.T.; Yuan, S.L.; Wang, W. Analysis of structural characteristics of typical check dam system in the third subregion of loess hilly region. *Res. Soil Water Conserv.* **2019**, *26*, 26–30. [CrossRef]
6. Wei, X.; Li, Z.B.; Wu, J.H.; Li, B.B.; Du, Z. A Discussion on some deological problems in research of water damage hazards of check dam. *Res. Soil Water Conserv.* **2007**, *14*, 235–237.
7. Zhang, Q.; Yang, J.H.; Wang, W.; Ma, P.L.; Lu, G.Y.; Liu, X.Y.; Yu, H.P.; Fang, F. Climatic Warming and Humidification in the Arid Region of Northwest China: Multi-Scale Characteristics and Impacts on Ecological Vegetation. *J. Meteorol. Res.* **2021**, *35*, 113–127. [CrossRef]
8. Zhang, Q.; Yang, J.H.; Duan, X.Y.; Ma, P.L.; Lu, G.Y.; Zhu, B.; Liu, X.Y.; Yue, P.; Wang, Y.H.; Liu, W.P. The eastward expansion of the climate humidification trend in northwest China and the synergistic influences on the circulation mechanism. *Clim. Dyn.* **2022**, *59*, 2481–2497. [CrossRef]
9. Ma, M.Y.; Wang, Q.M.; Liu, R.; Zhao, Y.; Zhang, D.Q. Effects of climate change and human activities on vegetation coverage change in northern China considering extreme climate and time-lag and -accumulation effects. *Sci. Total Environ.* **2023**, *860*, 160527–160540. [CrossRef]
10. Yang, S.P.; Zhao, G.P.; Mu, J.H.; Su, Z.S.; Ma, L.W.; Chen, X.J. Extreme Climatic Events and Its Effect in Ningxia. *J. Desert Res.* **2008**, *28*, 1169–1173.
11. Song, M.W.; Jiang, X.H.; Lei, Y.X.; Zhao, Y.R.; Cai, W.J. Spatial and temporal variation characteristics of extreme hydrometeorological events in the Yellow River Basin and their effects on vegetation. *Nat. Hazards* **2023**, *116*, 1863–1878. [CrossRef]
12. Huang, H.F.; Cui, H.J.; Ge, Q.S. Will a nonstationary change in extreme precipitation affect dam security in China. *J. Hydrol.* **2021**, *603*, 126859–126870. [CrossRef]

13. Iman, M.; Amir, A.K.; Mojtaba, S. Climate-Induced Changes in the Risk of Hydrological Failure of Major Dams in California. *Geophys. Res. Lett.* **2019**, *46*, 2130–2139. [CrossRef]
14. Du, Y.; Wang, D.G.; Zhu, J.X. Research on the Evolution of Warming and Humidification in Northwest China Based on CMIP5. *J. Water Resour. Water Eng.* **2021**, *32*, 61–69.
15. Zhang, B.; Liu, X.F.; Zheng, G.F.; Wang, F.; Wang, S.Y. Variation of the days of extreme precipitation in Ningxia in summer and its causes. *J. Atmos. Sci.* **2018**, *41*, 176–185. [CrossRef]
16. Kharin, V.V.; Zwiers, F.W.; Zhang, X.; Wehner, M. Changes in temperature and precipitation extremes in the CMIP5 ensemble. *Clim. Chang.* **2013**, *119*, 345–357. [CrossRef]
17. Qin, P.H.; Xie, Z.H.; Zou, J.; Liu, S.; Chen, S. Future Precipitation Extremes in China under Climate Change and Their Physical Quantification Based on a Regional Climate Model and CMIP5 Model Simulations. *Adv. Atmos. Sci.* **2021**, *38*, 460–479. [CrossRef]
18. Hay, L.E.; Wilby, R.L.; Leavesley, G.H. A Comparison of Delta Change and Downscaed GCM Scenarios for Three Mountainous Basins in the United States. *J. Am. Water. Resour. Assoc.* **2010**, *36*, 387–397. [CrossRef]
19. Gao, F.Q.; Zhao, X.Q. Delta method in large deviations and moderate deviations for estimators. *Ann. Stat.* **2011**, *39*, 1211–1240. [CrossRef]
20. Zhang, M.J.; Wang, B.L.; Wei, J.L.; Wang, S.J.; Ma, Q.; Li, X.F. Extreme event changes of air temperature in Ningxia in recent 50 years. *J. Nat. Disasters* **2012**, *21*, 152–160. [CrossRef]
21. Chen, X.G.; Conway, D.; Chen, X.J.; Zheng, G.F. Analysis of the Trend of Extreme Precipitation Events in Ningxia from 1961 to 2005. *Adv. Clim. Chang. Res.* **2008**, *4*, 156–160.
22. Li, F.; Zhang, M.J.; Li, X.F.; Wang, S.J.; Wang, Q.; Liu, W.L. Research on spatiotemporal evolution of extreme precipitation in Ningxia during 1962–2011. *J. Nat. Disasters* **2013**, *22*, 171–180. [CrossRef]
23. Yu, Y.; Hua, T.; Chen, L.; Zhang, Z.; Pereira, P. Divergent changes in vegetation greenness, productivity, and rainfall use efficiency are characteristic of ecological restoration towards high-quality development in the Yellow River Basin, China. *Engineering* **2023**. [CrossRef]
24. Fan, K.; Shi, H.L.; Chen, Y.X. Analysis on Characteristics of Precipitation Variation in Zhongwei City in Recent 50 Years. *Agric. Sci. Technol.* **2011**, *12*, 1917–1920. [CrossRef]
25. Xin, Z.B.; Xie, Z.R.; Wang, W. Character of Precipitation in Ningxia and Its Response to ENSO. *Sci. Geol. Sin.* **2005**, *25*, 49–55.
26. Ma, L.; Zhang, Q.F.; Ni, Y.X.; Li, M.; Lu, X.Z. Study on Siltation Depth in Warping Dam Under Different Silting Conditions in Chabagou Watershed. *Res. Soil Water Conserv.* **2022**, *29*, 18–22, 30. [CrossRef]
27. Baggio, T.; D'Agostino, V. Simulating the effect of check dam collapse in a debris-flow channel. *Sci. Total Environ.* **2022**, *816*, 151660–151671. [CrossRef] [PubMed]
28. Zu, Q.; Chen, Z.Y.; Yu, S.; Huang, X.P.; Yu, K.X.; Wang, Z.J.; Wang, L. Risk Analysis of Check Dam System Under Extreme Rainfall in Small Watershed. *J. Soil Water Conserv.* **2022**, *36*, 30–37. [CrossRef]
29. Liu, X.J.; Zhang, Y.; Xiao, T.Q.; Li, P.; Liu, Y.Q.; Deng, W.P. Runoff velocity controls soil nitrogen leaching in subtropical restored forest in Southern China. *For. Ecol. Manag.* **2023**, *548*, 121412–121420. [CrossRef]
30. Gao, Y.; Feng, Q.; Liu, W.; Lu, A.G.; Wang, Y.; Yang, J.; Cheng, A.G.; Wang, Y.M.; Su, Y.B.; Liu, L.; et al. Changes of daily climate extremes in Loess Plateau during 1960–2013. *Quat. Int.* **2015**, *371*, 5–21. [CrossRef]